

# Redox Behaviour of CeO<sub>2</sub> and Ce<sub>0.5</sub>Zr<sub>0.5</sub>O<sub>2</sub> Supported CuO Catalysts for CO Oxidation

Meng-Fei Luo\* and Xiao-Ming Zheng

Institute of Catalysis, Hangzhou University, Hangzhou 310028, PR China

Luo, M-F. and Zheng, X-M., 1998. Redox Behaviour of CeO<sub>2</sub> and Ce<sub>0.5</sub>Zr<sub>0.5</sub>O<sub>2</sub> Supported CuO Catalysts for CO Oxidation. – Acta Chem. Scand. 52: 1183–1187. © Acta Chemica Scandinavica 1998.

The reduction–oxidation behaviour of supported copper oxide catalysts has been investigated by temperature-programmed reduction. For the CuO/CeO<sub>2</sub> catalyst there are three reducible copper oxide species;  $\alpha$  and  $\beta$  peaks are attributed to the reduction of highly dispersed copper oxide species; a  $\gamma_1$  peak is ascribed to the reduction of bulk CuO. The order of reduction of three copper oxide species is found to be  $\alpha$ – $\beta$ – $\gamma_1$ , which is consistent with the order of reoxidation of copper species on a reduced CuO/CeO<sub>2</sub> catalyst. For the CuO/Ce<sub>0.5</sub>Zr<sub>0.5</sub>O<sub>2</sub> catalyst, three copper oxide species are also observed, an  $\alpha$  peak is attributed to the dispersed copper oxide species;  $\gamma_1$  and  $\gamma_2$  peaks are ascribed to the bulk CuO. The reduction of the CuO/CeO<sub>2</sub> catalyst is easier than for CuO/Ce<sub>0.5</sub>Zr<sub>0.5</sub>O<sub>2</sub>; the oxidation of the reduced CuO/CeO<sub>2</sub> catalyst is also easier than for the reduced CuO/Ce<sub>0.5</sub>Zr<sub>0.5</sub>O<sub>2</sub> catalyst. CuO dispersion on a CeO<sub>2</sub> support is larger than on Ce<sub>0.5</sub>Zr<sub>0.5</sub>O<sub>2</sub>. The catalytic activity of CuO/CeO<sub>2</sub> for CO oxidation is higher than that of CuO/Ce<sub>0.5</sub>Zr<sub>0.5</sub>O<sub>2</sub>, which is consistent with the dispersion and the reduction of CuO.

The oxidation of carbon monoxide is an important reaction in reducing air pollution, such as in automobile emission control. Many studies have shown that copper is a very active species.<sup>1,2</sup> Our previous study<sup>3</sup> has demonstrated that the CuO/CeO<sub>2</sub> catalyst exhibits high catalytic activity for CO oxidation, due to the combined effect of copper oxide and cerium dioxide. CO oxidation over copper-based catalysts is considered to proceed according to an oxidation–reduction mechanism of the active phase.<sup>4,5</sup> Jernigan and Somorjai<sup>6</sup> pointed out that CO oxidation over a CuO catalyst belongs to a redox cycle mechanism between CuO and Cu<sub>2</sub>O, and the rate-limiting step is the reduction of CuO by CO. Severino and Laine<sup>7</sup> also pointed out that CO oxidation over copper–chromium-based catalysts can be described by a redox cycle mechanism. Possible redox couples under reaction conditions are Cu<sup>+</sup>–Cu<sup>2+</sup>, Cu<sup>0</sup>–Cu<sup>2+</sup> and Cu<sup>0</sup>–Cu<sup>+</sup>. After calcination in air, copper is mainly present as Cu<sup>2+</sup>. The oxidation state of copper under oxygen-rich conditions is only slightly lower than Cu<sup>2+</sup>, which makes the redox couple Cu<sup>+</sup>–Cu<sup>2+</sup> the most probable for CO oxidation by oxygen.<sup>4,7</sup> Therefore, the redox cycle of copper species is very important for CO oxidation. In the present work, the reduction–oxidation behaviour of CeO<sub>2</sub> and Ce<sub>0.5</sub>Zr<sub>0.5</sub>O<sub>2</sub> supported CuO catalysts was investigated by means of the temperature-programmed reduction (TPR) technique.

\* To whom correspondence should be addressed.

## Experimental

**Preparation of catalysts.** The preparation of CuO/CeO<sub>2</sub> catalysts was described in our previous paper.<sup>3</sup> The Ce<sub>0.5</sub>Zr<sub>0.5</sub>O<sub>2</sub> support was prepared by evaporating an aqueous solution of the mixed metal nitrates containing an equivalent amount of citric acid to obtain a gel, followed by decomposition at 950 °C for 4 h. XRD (Fig. 6) indicates the formation of a single-phase Ce<sub>0.5</sub>Zr<sub>0.5</sub>O<sub>2</sub> solid solution (*d* values of diffraction peaks: 3.047, 2.640, 1.864, 1.589, 1.522). The BET surface areas of CeO<sub>2</sub> and Ce<sub>0.5</sub>Zr<sub>0.5</sub>O<sub>2</sub> are 55 and 11 m<sup>2</sup> g<sup>−1</sup>, respectively. The preparation of CuO/Ce<sub>0.5</sub>Zr<sub>0.5</sub>O<sub>2</sub> catalyst was the same as for the CuO/CeO<sub>2</sub> catalyst.

**Temperature-programmed reduction (TPR).** TPR was described in our previous paper,<sup>3</sup> and the heating rate of the TPR was 7 °C min<sup>−1</sup> in this work.

The purpose of the reoxidation treatment is to reveal the oxidation properties of the reduced catalyst. Before reoxidation, the catalyst was reduced with TPR. The reduction temperature was raised from room temperature to 400 °C and then held at 400 °C for 10 min. Subsequently the temperature of the catalyst was decreased to the desired temperature (i.e. 20, 100, 150, 200, 300 or 350 °C) and the gas flow was simultaneously switched to air for 1 h. Then the temperature of the catalyst was decreased to 20 °C. Finally, TPR of the reoxidation catalyst was carried out.

**Oxidation of CO.** Catalytic activity measurements were carried out in a fixed bed reactor (0.6 cm i.d.) using 150 mg of catalyst of 20–60 mesh size. The total gas flow rate was set at 80 ml min<sup>-1</sup>. The gas consisted of 2.4% CO and 1.2% O<sub>2</sub> in N<sub>2</sub>. The catalysts were directly exposed to 80 ml min<sup>-1</sup> of reaction gas as the reactor temperature stabilized at the reaction temperature, without any pretreatment. The analyses of the reactor effluent were performed with an on-line SP-2304 model gas chromatograph with a TCD attachment.

## Results and discussion

**Redox behaviour of CuO/CeO<sub>2</sub>.** Figure 1 shows the TPR profiles for CuO/CeO<sub>2</sub> catalysts with various Cu loadings. The reduction of pure CeO<sub>2</sub> begins at 400 °C (not shown in Fig. 1). The reduction profile of pure CuO is characterized by a single peak at 375 °C. From Fig. 1 it can be seen that when the copper loading is lower than 5%, two peaks are observed, and when the copper loading is higher than 5% a third peak is observed. The three peaks are designated by  $\alpha$ ,  $\beta$  and  $\gamma_1$  in Fig. 1. In our previous paper<sup>3</sup> only two TPR peaks were observed. The reason was that the heating rate in the previous paper<sup>3</sup> was 20 °C min<sup>-1</sup>, much larger than the 7 °C min<sup>-1</sup> in this work. The position of the  $\alpha$  and  $\beta$  peaks shifts to lower temperature, and the intensities increase with increasing copper loading. However, when the copper loading is higher than 5%, the position and intensity of  $\alpha$  and the peaks remain unchanged. As the copper loading increases above 5%, a third hydrogen consumption peak appears; moreover, its intensity increases rapidly with an increase in copper loading from 5 to 15%. The XRD results<sup>3</sup> show that when the copper loading is lower than 5%, no visible CuO crystal phases can be observed. As the CuO loading is increased, the crystal phase of CuO becomes apparent. Therefore, we propose that the  $\alpha$  and  $\beta$  species are represented by small

CuO particles which are finely dispersed, and on interacting with CeO<sub>2</sub> particles they are reduced at lower temperature. The  $\gamma_1$  species is represented by larger particle bulk CuO which reduces at a higher temperature.

The fluorite-type oxides, such as ceria and zirconia, have a face-centered-cubic crystal structure in which each tetravalent metal ion is surrounded by eight equivalent nearest O<sup>2-</sup> ions forming the vertices of a cube. Dow and Huang<sup>2</sup> have reported that when copper oxide is supported on YSZ (Y<sub>2</sub>O<sub>3</sub>-stabilized ZrO<sub>2</sub>), the interfacial terminal oxygen ion of copper oxide can be removed at very low temperature to form third and fourth TPR peaks, i.e.  $\alpha_1$  and  $\alpha_2$  peaks, as well as  $\beta$  and  $\gamma$  peaks. Two TPR peaks with lower peak temperatures (namely,  $\alpha_1$  and  $\alpha_2$ ) have been attributed to the hydrogen uptake of nested oxygen ions and temptable oxygen ions, respectively. The strong affinity between the surface oxygen vacancy ion of YSZ and the interface-boundary terminal oxygen ion of copper oxides will cause this Cu=O bond to be come weakened. Dow and Huang designated these oxygen ions as nested oxygen ions. The interface-boundary terminal oxygen ions which are in the vicinity of the surface oxygen vacancies of YSZ will be easily withdrawn by the corrosion of acid. These oxygen ions are temptable oxygen ions. The nested oxygen ion and temptable oxygen ion are interface-boundary terminal oxygen ions of the supported copper oxide but have different environment and interaction with the surface oxygen vacancies of the YSZ support. We believe that the  $\alpha$  and  $\beta$  peaks of our CuO/CeO<sub>2</sub> catalyst correspond to the  $\alpha_1$  and  $\alpha_2$  peaks of the CuO/YSZ catalyst in the literature.<sup>2</sup>

Figure 2 shows the TPR profiles of reoxidized CuO/CeO<sub>2</sub> (10% Cu loading) catalysts. All catalysts were oxidized for 1 h. From Fig. 2 it can be seen that only two lower temperature peaks ( $\alpha$  and  $\beta$ ) were observed. This indicates that the  $\alpha$  and  $\beta$  copper species were oxidized more easily than  $\gamma$  copper species. Comparison of Figs. 1 and 2 shows that reduction/oxidation treatment

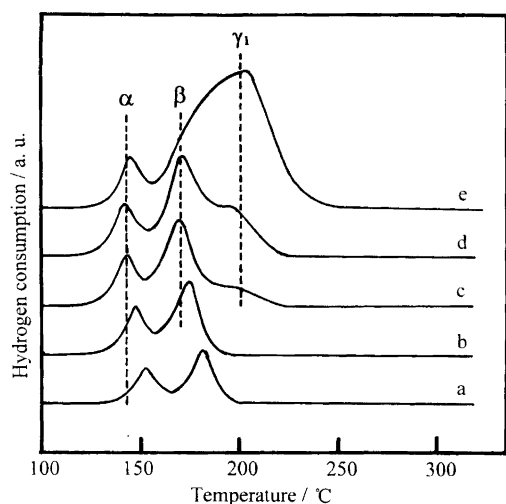


Fig. 1. TPR profiles of CuO/CeO<sub>2</sub> catalysts with various Cu loadings: (a) 2.0%; (b) 3%; (c) 5%; (d) 10%; (e) 15%.

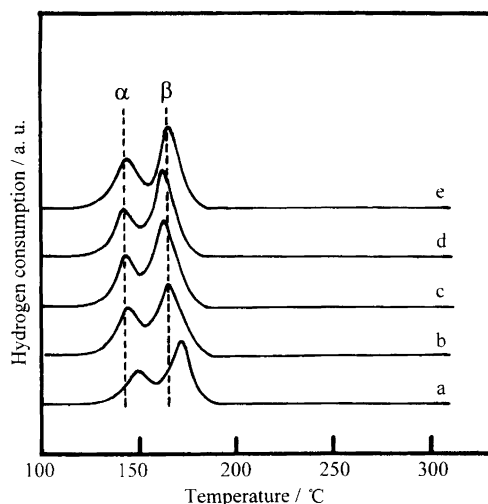


Fig. 2. TPR profiles of CuO/CeO<sub>2</sub> catalysts reoxidized at 20 °C. (a)–(e) as in Fig. 1.

promotes the reduction in reoxidized catalyst, since  $\alpha$  and  $\beta$  peak temperatures of the reoxidized samples are about 10 and 20 °C lower than that of the fresh samples, respectively. This indicates that reoxidation treatment promotes dispersion of the  $\alpha$  and  $\beta$  CuO species.

Figure 3 shows the effect of reoxidation temperature on the TPR profiles of reoxidized  $\text{CuO/CeO}_2$  (10% Cu loading) catalyst. It can be seen that when  $\text{CuO/CeO}_2$  was oxidized by 5%  $\text{O}_2$  for 15 min at 20 °C, only the  $\alpha$  peak is observed. As the temperature of reoxidation treatment increases,  $\beta$  and  $\gamma_1$  peaks appear successively. This indicates that the order of reoxidation of three copper species is  $\alpha$ – $\beta$ – $\gamma_1$ , which is consistent with the order of reduction of three copper oxide species ( $\alpha$ ,  $\beta$  and  $\gamma_1$ ).

**Redox behaviour of  $\text{CuO/Ce}_{0.5}\text{Zr}_{0.5}\text{O}_2$ .** Figure 4 shows the TPR profiles of  $\text{CuO/Ce}_{0.5}\text{Zr}_{0.5}\text{O}_2$  catalyst with various Cu loadings. The intensity of the  $\gamma_1$  and  $\gamma_2$  peaks increases appreciably with copper loading, while the  $\alpha$  peak does not change. The reduction behaviour of the  $\text{CuO/Ce}_{0.5}\text{Zr}_{0.5}\text{O}_2$  catalyst is thus obviously different from that of  $\text{CuO/CeO}_2$ . The reduction temperature of  $\text{CuO/Ce}_{0.5}\text{Zr}_{0.5}\text{O}_2$  is higher than that of  $\text{CuO/CeO}_2$ . Only one peak is observed below 200 °C, with two peaks above 200 °C. Figure 5 shows the XRD patterns of  $\text{CuO/CeO}_2$  (10%) and  $\text{CuO/Ce}_{0.5}\text{Zr}_{0.5}\text{O}_2$  catalysts. Very weak CuO diffraction peaks can be observed in both  $\text{CuO/CeO}_2$  (10%) and  $\text{CuO/Ce}_{0.5}\text{Zr}_{0.5}\text{O}_2$  (2%) catalysts. However, CuO diffraction peaks can be observed in  $\text{CuO/Ce}_{0.5}\text{Zr}_{0.5}\text{O}_2$  (5%) and  $\text{CuO/Ce}_{0.5}\text{Zr}_{0.5}\text{O}_2$  (10%) catalysts. This shows that the  $\text{CuO/CeO}_2$  catalyst has a higher CuO dispersion than  $\text{CuO/Ce}_{0.5}\text{Zr}_{0.5}\text{O}_2$ . This may be related to the BET surface area of these supports; the BET surface area of  $\text{CeO}_2$  ( $55 \text{ m}^2 \text{ g}^{-1}$ ) is higher than that of  $\text{Ce}_{0.5}\text{Zr}_{0.5}\text{O}_2$  ( $11 \text{ m}^2 \text{ g}^{-1}$ ). Zheng *et al.*<sup>8</sup> and Lu

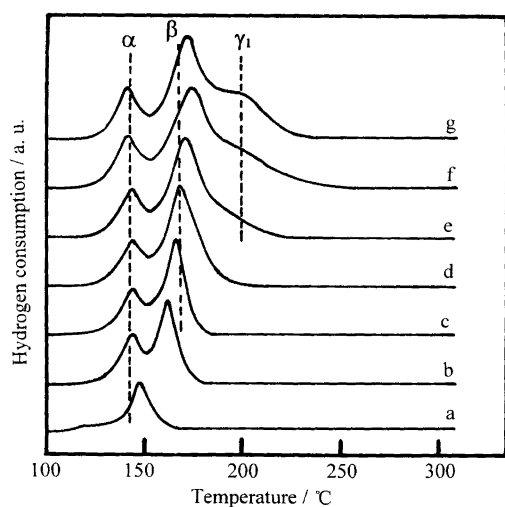


Fig. 3. TPR profiles of  $\text{CuO/CeO}_2$  (10%) catalyst reoxidized at different temperatures in 5%  $\text{O}_2$  or air: (a) reoxidized at 20 °C in 5%  $\text{O}_2$ ; (b) 20 °C in air; (c) 100 °C in air; (d) 150 °C in air; (e) 200 °C in air; (f) 300 °C in air; (g) fresh catalyst.

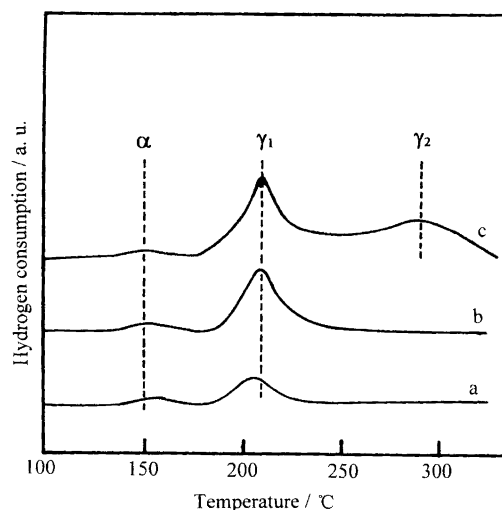


Fig. 4. TPR profiles of  $\text{CuO/Ce}_{0.5}\text{Zr}_{0.5}\text{O}_2$  catalysts with various Cu loadings: (a) 2.0%; (b) 5%; (c) 10%.

*et al.*<sup>9</sup> report that CuO and NiO on the support surface exist in both crystalline and non-crystalline (dispersed metal oxide). The amount of non-crystalline CuO has a threshold limit value which was determined by the properties and surface area of the support. Because  $\text{Ce}_{0.5}\text{Zr}_{0.5}\text{O}_2$  has an identical structure to  $\text{CeO}_2$ , we believe the surface area of the support plays a leading role. On the basis of the XRD result, we believe that the  $\alpha$  peak is the dispersed copper oxide, while the  $\gamma_1$  and  $\gamma_2$  peaks are bulk CuO.

Figure 6 shows the TPR profiles of fresh and reoxidized  $\text{CuO/Ce}_{0.5}\text{Zr}_{0.5}\text{O}_2$  (10%) catalyst with different reoxidation temperatures. When the reduced  $\text{CuO/Ce}_{0.5}\text{Zr}_{0.5}\text{O}_2$  catalyst was oxidized at 20 and 100 °C, only the lower temperature peak is observed, the temperature of the peak is about 170 °C, which is higher than that of the  $\alpha$  peak of fresh  $\text{CuO/Ce}_{0.5}\text{Zr}_{0.5}\text{O}_2$  catalyst. As the temperature of reoxidation treatment increases, an overlap peak is clearly seen, the intensity of the reduction peak increases and the peak positions shift to higher temperatures, but  $\alpha$  and  $\gamma_2$  peaks do not appear even with oxidation at 350 °C. The area of the overlap peak of the reoxidized catalyst is about the same as the area of the  $\alpha + \gamma_1 + \gamma_2$  peak of the fresh catalyst. By comparison with Fig. 3, it can be seen that the reduced  $\text{CuO/Ce}_{0.5}\text{Zr}_{0.5}\text{O}_2$  catalyst is more difficult to oxidize than the reduced  $\text{CuO/CeO}_2$  catalyst. On the basis of above result, we conclude that reduction of the  $\text{CuO/CeO}_2$  catalyst is easier than that of  $\text{CuO/Ce}_{0.5}\text{Zr}_{0.5}\text{O}_2$ , and oxidation of the reduced  $\text{CuO/CeO}_2$  catalyst is also easier than that of reduced  $\text{CuO/Ce}_{0.5}\text{Zr}_{0.5}\text{O}_2$  catalyst.

**Catalytic activity for CO oxidation.** Figure 7 shows the CO oxidation conversion over  $\text{CuO/CeO}_2$ , and  $\text{CuO/Ce}_{0.5}\text{Zr}_{0.5}\text{O}_2$  catalysts. At each reaction temperature, the reaction was continued for about 1 h to achieve steady-state activity. From Fig. 7 it can be seen that CO

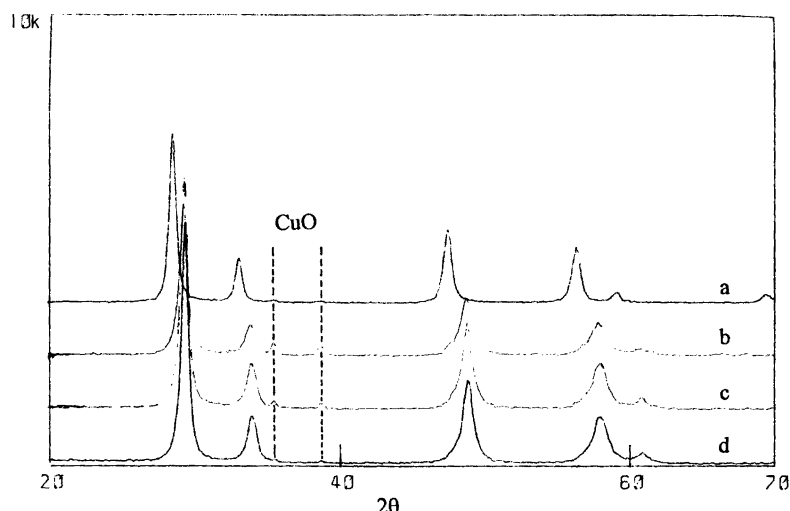


Fig. 5. XRD pattern of CuO/CeO<sub>2</sub> and CuO/Ce<sub>0.5</sub>Zr<sub>0.5</sub>O<sub>2</sub> catalysts: (a) CuO/CeO<sub>2</sub> (10%); (b) CuO/Ce<sub>0.5</sub>Zr<sub>0.5</sub>O<sub>2</sub> (10%); (c) CuO/Ce<sub>0.5</sub>Zr<sub>0.5</sub>O<sub>2</sub> (5%); (d) CuO/Ce<sub>0.5</sub>Zr<sub>0.5</sub>O<sub>2</sub> (2%).

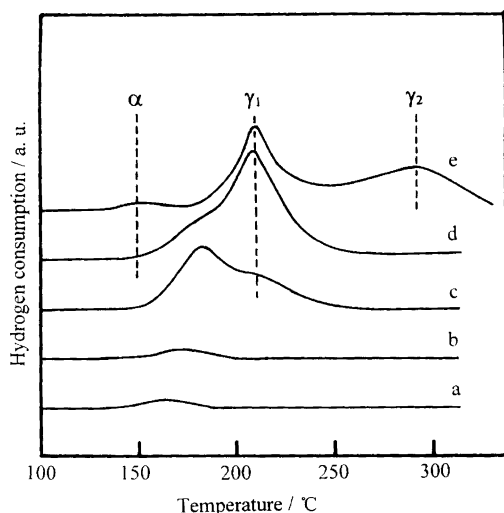


Fig. 6. TPR profiles of CuO/Ce<sub>0.5</sub>Zr<sub>0.5</sub>O<sub>2</sub> catalysts reoxidized at different temperatures in air. (a) 20; (b) 100; (c) 200; (d) 350 °C; (e) fresh catalyst.

conversion of 90% over the CuO/CeO<sub>2</sub>, and CuO/Ce<sub>0.5</sub>Zr<sub>0.5</sub>O<sub>2</sub> catalysts takes place at 60 and 120 °C, respectively. This indicates the CuO/CeO<sub>2</sub> catalyst shows much higher activity than CuO/Ce<sub>0.5</sub>Zr<sub>0.5</sub>O<sub>2</sub> catalyst. The support has a significant effect on the activity of the supported CuO catalyst. On the basis of the TPR and XRD results, we believe that the reason for the high activity of CuO/CeO<sub>2</sub> catalyst is the high surface area of the CeO<sub>2</sub> support. The α and β peaks are responsible for low-temperature CO oxidation. The high surface area is not only advantageous to the dispersion of CuO species but also increases the content of dispersed CuO on the support surface. Thus the activity of the CuO/CeO<sub>2</sub> catalyst is much higher than that of the CuO/Ce<sub>0.5</sub>Zr<sub>0.5</sub>O<sub>2</sub> catalyst.

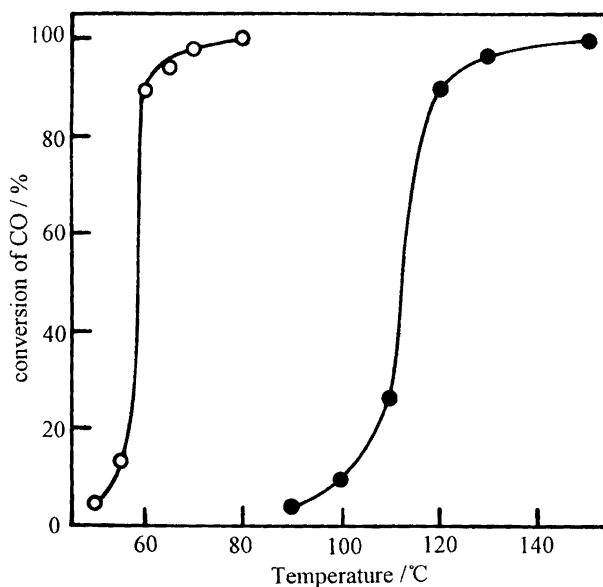


Fig. 7. CO oxidation over (○) CuO/CeO<sub>2</sub> (10%) and (●) CuO/Ce<sub>0.5</sub>Zr<sub>0.5</sub>O<sub>2</sub> (10%) catalysts.

### Conclusions

CuO/CeO<sub>2</sub> and CuO/Ce<sub>0.5</sub>Zr<sub>0.5</sub>O<sub>2</sub> catalysts have been prepared using impregnation methods. The reduction-oxidation behaviour of CuO/CeO<sub>2</sub> and CuO/Ce<sub>0.5</sub>Zr<sub>0.5</sub>O<sub>2</sub> catalysts was investigated by TPR. Three TPR peaks on CuO/CeO<sub>2</sub> and CuO/Ce<sub>0.5</sub>Zr<sub>0.5</sub>O<sub>2</sub> catalysts can be observed. For CuO/CeO<sub>2</sub> catalysts, α and β peaks are attributed to the reduction of highly dispersed copper oxide species; a γ<sub>1</sub> peak is ascribed to the reduction of bulk CuO. The order of reduction of the three copper oxide species is found to be α-β-γ<sub>1</sub>, which is consistent with the order of reoxidation of copper oxide species. For CuO/Ce<sub>0.5</sub>Zr<sub>0.5</sub>O<sub>2</sub> catalysts, the α peak is dispersed CuO, while the γ<sub>1</sub> and γ<sub>2</sub> peaks are bulk CuO.

The reoxidation behaviour of CuO/Ce<sub>0.5</sub>Zr<sub>0.5</sub>O<sub>2</sub> is different from that of CuO/CeO<sub>2</sub>. After oxidation at 350 °C, the  $\alpha$  and  $\gamma_2$  peaks do not appear, but an overlap peak is observed. CuO dispersion on CeO<sub>2</sub> supports is larger than on CuO/Ce<sub>0.5</sub>Zr<sub>0.5</sub>O<sub>2</sub>. The catalytic activity of CuO/CeO<sub>2</sub> for CO oxidation is higher than that of CuO/Ce<sub>0.5</sub>Zr<sub>0.5</sub>O<sub>2</sub>. However, a study of systems with more comparable BET surface areas would be desirable.

*Acknowledgment.* This work was supported by the Zhejiang Provincial Natural Science Foundation of China.

## References

1. Dow, W.-P. and Huang, T.-J. *J. Catal.* 147 (1994) 322.
2. Liu, W. and Flytani-Stephanopoulos, M. *J. Catal.* 153 (1995) 304.
3. Luo, M.-F., Zhong, Y.-J., Yuan, X.-X. and Zheng, X.-M. *Appl. Catal. A* 162 (1997) 121.
4. Dekker, N. J. J., Hoorn, A. J. J., Stegenga, S., Kapteijn, F. and Moulijn, J. A. *Am. Inst. Chem. Eng. J.* 38 (1992) 385.
5. Miro, E. E., Lombardo, E. A. and Pentunichi, J. O. *J. Catal.* 104 (1987) 176.
6. Jernigan, G. G. and Somorjai, G. A. *J. Catal.* 147 (1994) 567.
7. Severino, F. and Laine, J. *Ind. Eng. Chem. Prod. Res. Dev.* 22 (1983) 396.
8. Zheng, Y.-F., Xian, Y.-C., Zheng, Y., Zheng, D.-L. and Tang, Y.-Q. *J. Sci. Sinica, Ser. B* 8 (1986) 805.
9. Lu, G.-L. Chen, L.-S., Lin, R.-G., Huang, S.-M. and Tang, X.-S. *J. Hangzhou Univ.* 17 (1990) 314.

Received January 21, 1998.